Polyelectrolyte Brush Interacting with Ampholytic Nanoparticles as Coarse-Grained Models of Globular Proteins: Poisson–Boltzmann Theory

Tatiana O Salamatova, Mikhail Y Laktionov, Ekaterina B Zhulina, Oleg V. Borisov

BioMACROMOLECULES

pubs.acs.org/Biomac

Article

Polyelectrolyte Brush Interacting with Ampholytic Nanoparticles as Coarse-Grained Models of Globular Proteins: Poisson−Boltzmann Theory

Tatiana O. Salamatova, Mikhail Y. Laktionov, Ekaterina B. Zhulina, and Oleg V. Borisov*

Cite This: https://doi.org/10.1021/acs.biomac.2c01153

Read Online

ACCESS | Metrics & More | Article Recommendations | Supporting Information

ABSTRACT: The self-consistent field Poisson−Boltzmann framework is applied to analyze equilibrium partitioning of ampholytic nanoparticles (NPs) between buffer solution and polyelectrolyte (PE) polyanionic brush. We demonstrate that depending on pH and salt concentration in the buffer solution, interactions between ionizable (acidic and basic) groups on the NP surface and electrostatic field created by PE brush may either lead to the spontaneous uptake of NPs or create an electrostatic potential barrier, preventing the penetration of NPs inside PE brush. The capability of PE brush to absorb or repel NPs is determined by the shape of the insertion free energy that is calculated as a function of NP distance from the grafting surface. It is demonstrated that, at a pH value below or slightly above the isoelectric point (IEP), the electrostatic free energy of the particle is negative inside the brush and absorption is thermodynamically favorable. In the latter case, the insertion free energy exhibits a local maximum (potential barrier) at the entrance to the brush. An increase in pH leads to the shallowing of the free energy minimum inside the brush and a concomitant increase in the free energy maximum, which may result in kinetic hindering of NP uptake. Upon further increase in pH the insertion free energy becomes positive, making NP absorption thermodynamically unfavorable. An increase in salt concentration diminishes the depth of the free energy minimum inside the brush and eventually leads to its disappearance. Hence, in accordance with existing experimental data our theory predicts that an increase in salt concentration suppresses absorption of NPs (protein globules) by PE brush in the vicinity of IEP. The interplay between electrostatic driving force for NP absorption and osmotic repelling force (proportional to NP volume) indicates that for large NPs with relatively small number of ionizable groups osmotic repulsion overcomes electrostatic attraction preventing thereby absorption of NPs by PE brush.

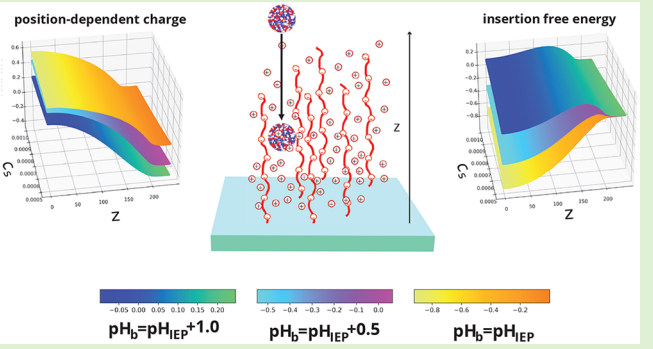

1. INTRODUCTION

Electrostatic interactions between charged biomacromolecules and proteins play an important role in many biological processes.[1−4] A better understanding of the interactions between natural polyelectrolytes and proteins could thus have both fundamental scientific importance and direct medical implications. Synthetic polyelectrolytes (PEs) and colloidal polyelectrolyte nanostructures could mimic natural polyelectrolytes and their assemblies to unravel mechanisms of molecular processes in living nature, including those of direct medical relevance (e.g., inflammation or coagulation cascades). On the other hand, colloidal PE nanostructures, such as polyelectrolyte brushes, microgels, or block polyelectrolyte micelles can be used in medical and biotechnological applications (e.g., drug and gene delivery, inhibition of viral infection, etc.).[5−14]

PE brushes (layers of charged macromolecules terminally attached to a planar substrate or to the surface of colloidal particles and immersed in aqueous solution) play a prominent role here, and their interactions with charged species have been actively explored experimentally and theoretically (see ref 1 for a comprehensive review). Planar, spherical, and cylindrical PE brushes are distinguished according to the geometry of the grafting surface. The latter closely mimic natural glycosaminoglycans (GAGs) (e.g., aggrecan in articular cartilage, envisioned as a cylindrical brush with keratan sulfate and chondroitin sulfate side chains end-tethered to the core protein[15]), or heparan-sulfate proteoglycans (HSPG) emanating from the cell surface.[16]

In living systems, globular proteins interact with charged biomacromolecular assemblies that often have complex brush-

Received: September 22, 2022
Revised: March 21, 2023

like architectures (e.g., layers of bacterial extracellular polysaccharides, endothelial glycocalyx, complexes of aggrecanes with hyaluronic acid, etc.) comprising both weak (carboxyl) and strong (sulfate) anionic groups. Synthetic PE brushes can be formed by macromolecules comprising either strong (permanently charged) or weak (pH-sensitive) ionizable groups. Proteins, on the other hand, are weak polyampholytes (PAs) that bear pH-sensitive cationic and anionic groups on their surface. Hence, the net charge of the protein globule depends on pH, and vanishes in the so-called isoelectric point, pH_{IEP}, in which the net charges of cationic and anionic groups exactly match each other. Hence, the protein globule possesses a net positive or negative charge at $pH \leq pH_{IEP}$ or $pH \geq pH_{IEP}$, respectively.

Under physiological conditions, biomacromolecular brushes and most of globular proteins are similarly (negatively) charged, so that their interactions could be mediated by the Coulomb electrostatic repulsions. On the other hand, seminal works of M. Ballauff and co-workers convincingly demonstrated that synthetic polyanionic brushes can efficiently uptake globular proteins above (on the "wrong side") the IEP, that is, when the PE brush and the protein are both negatively charged.[17−20] It was also demonstrated that absorption of the proteins is efficient at low and suppressed at high ionic strength due to the electrostatic nature of attraction between similarly (negatively) charged PE brushes and proteins.

Two possible mechanisms were proposed to explain this experimental observation: First, it was suggested that, due to the Donnan equilibrium, pH inside the polyanionic brush may be lower than pH_{IEP} even when pH in the buffer is higher than pH_{IEP} so that the protein which is negatively charged in the buffer, acquires positive charge inside the negatively charged brush and, therefore, is spontaneously absorbed by the brush.[21−23] An alternative hypothesis exploits the fact that cationic and anionic groups on the protein globule surface are distributed inhomogeneously and give rise to "patches" of positive and negative charges. Even when in total the globule is charged negatively, adsorption of the brush-forming polyanions on the (minority) patches of positive charge leads to the gain in the electrostatic free energy which overcompensates the free energy losses due to depletion from the negatively charged patches.[24,25] Recent experiments on complexation between polyelectrolytes and green fluorescent protein mutants with varied patchiness in the surface charge distribution[26] convincingly supports the importance of this mechanism of polyelectrolyte−protein binding. Both hypotheses provide qualitatively plausible explanation of the protein absorption by similarly charged PE brushes though both lack quantitative theoretical justification. Presumably, the reionization may serves as the dominant driving force for binding of proteins with fairly uniform (nonpatchy) distribution of cationic and anionic groups on the globule surface, by strongly charged PE brushes, including biological ones (e.g., HSPG). This is in a line with results of numerical self-consistent field calculations for protein-like ampholytic particles interacting with planar PE brushes[23] and molecular dynamics simulations of short ampholytic molecules interacting with a starlike PE.[27] At the same time, the short-range nonelectrostatic interactions between protein amino acid residues and the brush monomer units could also be significant, and in a general case, absorption of proteins by PE brushes is governed by both types of interactions.[20]

In our recent paper[28] we have demonstrated that charge inversion due to reionization of a weak ampholytic nanoparticle (NP) upon insertion into a similarly charged PE brush or microgel is a necessary but insufficient condition for the negative balance in the differential free energy. In other words, even if the NP, being negatively charged in the buffer, acquires a positive charge inside the negatively charged brush, the net ionic interaction balance may disfavor its uptake by the brush. This qualitative conclusion was made on the basis of a simple Donnan model that disregards the spatial distribution of an electrostatic field inside the PE brush/microgel.

Advances in the theory of polyelectrolyte brushes[29,30,32] provide a full quantitative analytical description of the electrostatic potential and local concentrations of mobile ions inside and outside of planar PE brushes within the accuracy of the Poisson−Boltzmann approximation. This theoretical approach has been recently extended[33] to brushes formed by branched polyelectrolytes that mimic natural biomacromolecular brushes, and can be applied with reasonable accuracy to PE brushes on surfaces of large colloidal particles.[34]

In this study, we focus exclusively on the electrostatic driving forces with aim to unravel different mechanisms regulating uptake of nanoparticles and globular proteins by PE brushes. We assimilate globular proteins to weak polyampholytic nanoparticles (NPs) with fixed volume and surface area covered with both acidic and basic ionizable groups. Although such coarse-graining of globular proteins is rather reductionistic, it could still illuminate general trends in the electrostatic regulation of the protein-PE brush interactions. The aim of the present paper is to implement the Poisson−Boltzmann framework to analyze the position-dependent ionization and insertion free energy of weak (pH-sensitive) polyampholytic NPs, and to examine the effect of environmental conditions (pH, salt concentration) and the brush grafting density on the shape of insertion free energy curves. This approach provides the distribution profiles of NPs inside the brush and may be further used to access the diffusion rates of NPs through PE brushes.

The rest of the paper is organized as follows: In section 2 we introduce our theoretical model and present dominant contributions to the NP free energy in the brush. A brief summary on the Poisson−Boltzmann theory of PE brushes and the review of electrostatic potential distribution is given in section 3, while more detailed derivations are delegated to the SI. Sections 3.1 and 3.2 are devoted to formulation of the electrostatic and osmotic contributions to the insertion free energy, respectively. The insertion free energy profiles calculated under varied conditions for NPs with one anionic and one cationic type of ionizable sites are presented in section 3.3. Finally, in section 4 we overview the results and outline our conclusions.

2. METHOD

2.1. Model. We consider a polyampholytic nanoparticle (NP), as a model of a protein in its globular conformation, that comprises N_+ ionogenic groups (sites) capable of acquiring positive (elementary) charge upon protonation, and N_- monomer units capable of acquiring negative (elementary) charge upon dissociation of hydrogen ion. The NP has volume V and ionizable groups are assumed to be evenly distributed on its surface with area Σ.

https://doi.org/10.1021/acs.biomac.2c01153
Biomacromolecules XXXX, XXX, XXX−XXX

In the general case, the NP might contain several types of cationic and anionic ionogenic groups (i.e., amino acid residues), each characterized by specific acidic ionization constant $K_{i\pm}$. We ascribe the ionization constant K_{i-} to N_{i-} anionic groups ($i_- = 1, 2, ...$) and the ionization constant K_{i+} to N_{i+} cationic groups ($i+ = 1, 2, ...$). Hence, the total number of ionizable groups is

$$N_\Sigma = N_+ + N_- = \sum_{i+} N_{i+} + \sum_{i-} N_{i-} \quad (1)$$

The NP is interacting with a polyelectrolyte brush, Figure 1. The brush is formed by strong (quenched) polyelectrolytes

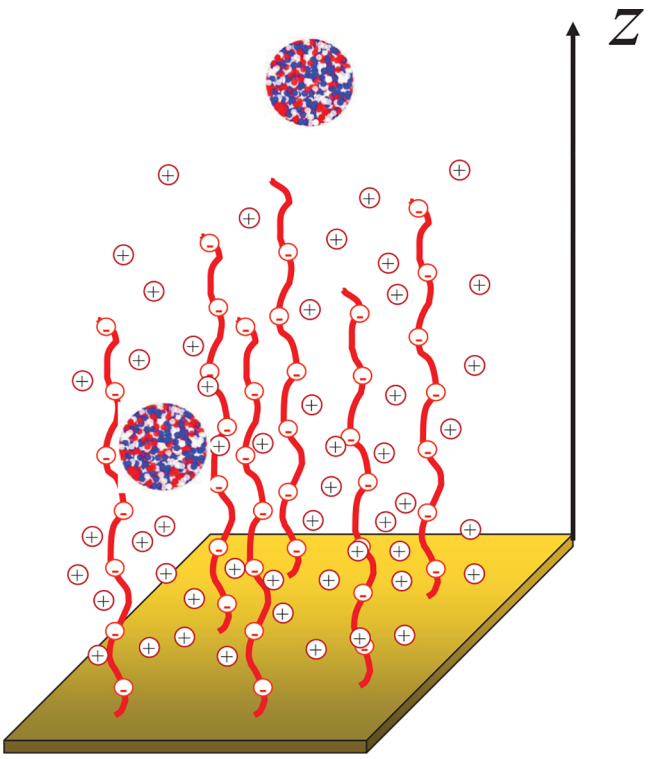

Figure 1. Schematics of an ampholytic NP insertion into a polyelectrolyte brush. Blue, red, and white areas on the globule surface correspond to cationic, anionic, and neutral residues, respectively.

(polyacids) with degree of polymerization $\mathcal{N} \gg 1$ end-tethered to the surface with density $\sigma = a^2/s$ (a is length of monomer unit and s is the grafting area per chain). The PE chains are assumed to be intrinsically flexible (with Kuhn segment length on the order of monomer unit length, a), and have a fraction α of (negatively) charged monomer units.

The pH in the solution (in the buffer) is fixed to the value of pH_b. The solution contains monovalent (positively and negatively charged) mobile ions of low molecular weight salt with concentration (number density)

$$c_{b+} = c_{b-} = c_s \quad (2)$$

that controls the Debye screening length

$$\kappa^{-1} = (8\pi l_B c_s)^{-1/2} \quad (3)$$

Here, $l_B = e^2/\epsilon k_B T$ is the Bjerrum length (e is the elementary charge, ϵ is the dielectric permittivity of the solvent, k_B is the Boltzmann constant, and T is the temperature). In the following we assume that $l_B = a$, which leads to the proportionality factor ≈5 between molar concentration and volume fraction $C_s = c_s a^3$ of the salt ions.

Because of excess electrostatic potential $\Psi(z) \le 0$ created by PE brush at distance z from the grafting surface (with the reference value $\Psi(z = \infty) = 0$), and respective gradient in the local concentration of hydrogen ions, the replacement of the NP from buffer solution into PE brush at distance z is accompanied by reionization of its cationic and anionic groups, and leads to the concomitant change in the NP free energy,

$$\Delta F(z) = \Delta F_{ion}(z) + \Delta F_{vol}(z) \quad (4)$$

Here, $\Delta F_{ion}(z)$ and $\Delta F_{vol}(z)$ account for reionization free energy and for the work against excess osmotic pressure inside the brush, respectively.

2.2. Electrostatic Potential of a Quenched Polyelectrolyte Brush. The reduced self-consistent electrostatic potential, $\psi(z) \equiv e\Psi(z)/k_B T$, in a negatively charged (anionic) PE brush can be presented as

$$\psi_{in}(z) = \frac{z^2 - H^2}{H_0^2} + \psi_{in}(H), \quad 0 \le z \le H \quad (5)$$

Here, z is the distance from the grafting surface, H is the total thickness of the brush (cutoff of the polymer density profile), and H_0 is the characteristic length

$$H_0/a = \sqrt{\frac{8}{3\pi^2}}\mathcal{N}\alpha^{1/2} \quad (6)$$

The value of constant $\psi_{in}(H)$ depends on the potential calibration, and ensures continuity of the potential at the brush edge, $\psi_{in}(H) = \psi_{out}(H)$. The potential outside the brush, $\psi_{out}(z)$, coincides with that of a uniformly charged plane with the surface charge per unit area equal to the residual (negative) charge per unit area of the brush

$$\tilde{q} = \int_0^H \rho(z)dz = -\frac{H}{2\pi l_B H_0^2} \quad (7)$$

with the residual charge density $\rho(z)$ specified by the Poisson equation,

$$\frac{d^2\psi_{in}(z)}{dz^2} = -4\pi l_B \rho(z) \quad (8)$$

(Here and below, charge is measured in the elementary charge, e, units.) The electrostatic potential outside the brush is thus formulated as[30]

$$\psi_{out}(z) = -2\ln\left[\frac{(\kappa\tilde{\Lambda} + \sqrt{(\kappa\tilde{\Lambda})^2 + 1} - 1) + (\kappa\tilde{\Lambda} - \sqrt{(\kappa\tilde{\Lambda})^2 + 1} + 1)e^{-\kappa(z-H)}}{(\kappa\tilde{\Lambda} + \sqrt{(\kappa\tilde{\Lambda})^2 + 1} - 1) - (\kappa\tilde{\Lambda} - \sqrt{(\kappa\tilde{\Lambda})^2 + 1} + 1)e^{-\kappa(z-H)}}\right] \quad (9)$$

with the Gouy−Chapman length

https://doi.org/10.1021/acs.biomac.2c01153
Biomacromolecules XXXX, XXX, XXX−XXX

$$\tilde{\Lambda} = \frac{1}{2\pi l_B |\tilde{q}|} = \frac{H_0^2}{H} \tag{10}$$

The latter controls distributions of the electrostatic potential and small mobile ions outside the brush, i.e., at $z \geq H$. The potential defined by eq 9 vanishes at $z \to \infty$. The cutoff of the polymer density profile, $z = H$, is found from the condition of conservation of number of monomer units in grafted chains. The minimal value reached by the electrostatic potential at the grafting surface, $z = 0$,

$$\psi_{in}(0) = -\frac{H^2}{H_0^2} + \psi(H) = -\frac{H^2}{H_0^2} + 2\ln\left[\frac{\sqrt{(\kappa\tilde{\Lambda})^2 + 1} - 1}{\kappa\tilde{\Lambda}}\right] \tag{11}$$

is the increasing function of salt concentration c_s in the buffer but the decreasing function of the grafting density σ. However, the potential difference across the brush,

$$-\psi_{in}(0) + \psi(H) = \frac{H^2}{H_0^2} \tag{12}$$

decreases as a function of salt concentration and increases upon an increase in the grafting density, because the brush thickness H decreases as a function of salt concentration, but increases as a function of σ.

The polymerization degree $\mathcal{N}$ of the grafted PE chains weakly affects $\psi(0)$, while the brush thickness $H \sim \mathcal{N}$. More detailed derivation and typical shapes of the electrostatic potential profile inside and outside the brush are presented in SI.

Notably, the parabolic shape of electrostatic potential $\psi_{in}(z)$ in eq 5 holds if the stretched brush-forming chains are still far from full extension (i.e., $H \leq L = a\mathcal{N}$). An approach to full extension of the tethered PE chains ($H \to L$) modifies electrostatic potential $\psi_{in}(z)$ as[31]

$$\psi_{in}(z) = \frac{3}{\alpha}\ln\frac{\cos(\pi z/2L)}{\cos(\pi H/2L)}$$

Electrostatic potential $\psi_{out}(z)$ outside strongly stretched PE brush is given by eq 9 with renormalized Gouy−Chapman length

$$\tilde{\Lambda} = \frac{H_0^2}{H}\frac{(\pi H/2L)}{\tan(\pi H/2L)}$$

In the following we assume that the tethered PEs are moderately charged (with degree of ionization $\alpha < 1$) to ensure the parabolic shape of $\psi_{in}(z)$.

3. RESULTS AND DISCUSSION

3.1. Ionic Contribution to the Free Energy. Transfer of NP from the bulk of solution in PE brush is accompanied by the change in ionization states of both basic and acidic groups on NP surface. The ionic part of the differential free energy can be expressed as[28]

$$\Delta F_{ion}(z)/k_BT = \sum_{i+} N_{i+}\ln\left(\frac{1-\alpha_{i+}(z)}{1-\alpha_{bi+}}\right) + \sum_{i-} N_{i-}\ln\left(\frac{1-\alpha_{i-}(z)}{1-\alpha_{bi-}}\right) \tag{13}$$

where α_{bi+}, $\alpha_{i+}(z)$, α_{bi-}, and $\alpha_{i-}(z)$ are the respective degrees of ionization of basic and acidic monomer units on the surface of NP placed at distance z from the grafting surface and in the bulk of the solution (at $z = \infty$).

Here,

$$\alpha_{i+}(z) = (1 + K_{i+}/[H^+(z)])^{-1} \equiv (1 + 10^{pH(z)-pK_{i+}})^{-1} = \left(1 + \frac{1-\alpha_{bi+}}{\alpha_{bi+}}\exp(\psi(z))\right)^{-1} \tag{14}$$

and

$$\alpha_{i-}(z) = (1 + [H^+(z)]/K_{i-})^{-1} \equiv (1 + 10^{pK_{i-}-pH(z)})^{-1} = \left(1 + \frac{1-\alpha_{bi-}}{\alpha_{bi-}}\exp(-\psi(z))\right)^{-1} \tag{15}$$

The respective degrees of ionization of ionogenic groups $i\pm$ in the buffer are

$$\alpha_{bi+} = (1 + K_{i+}/[H^+]_b)^{-1} = (1 + 10^{pH_b-pK_{i+}})^{-1} \tag{16}$$

and

$$\alpha_{bi-} = (1 + [H^+]_b/K_{i-})^{-1} = (1 + 10^{pK_{i-}-pH_b})^{-1} \tag{17}$$

$[H^+(z)]$ is the local concentration of hydrogen ions (specifying local $pH(z) = -\log[H^+(z)]$), $pH_b \equiv pH(z = \infty) = -\log[H^+(z = \infty)]$, and K_{i+} and K_{i-} are respective acidic ionization constants of basic and acidic groups.

According to eqs 14 and 15, ionization of acidic and basic ionogenic groups is controlled by local electrostatic potential $\psi(z)$ in the brush, while the Coulomb interactions between ionized groups on NP surface are disregarded. These interactions could shift the ionization constants with respect to "bare" constants K_{i+} and K_{i-} (see refs 35 and 36). Within the applied here approximation, $\{N_{i\pm}\}$ and $\{K_{i\pm}\}$ are considered as independent sets of variables. We also neglect the electrostatic potential gradient on the length scale of NP spatial dimensions.

The spacial distribution of hydrogen ions can be expressed as

$$[H^+(z)] = [H^+]_b \exp(-\psi(z)) \tag{18}$$

As long as hydrogen ions are distributed between PE brush and solution according to eq 18, lower electrostatic potential inside the brush, $\Psi(z) \leq 0$, indicates that local concentration of H^+ ions inside the brush is larger than in the bulk of the solution. As a result, the degree of ionization of basic residues inside polyanionic brush is higher, while the degree of ionization of acidic residues is lower than in the bulk of the solution (eqs 14 and 15). The sign of $\Delta F_{ion}(z)$ is determined by the balance between reionization free energies of basic and acidic monomer units (the first and the second terms in eq 13, respectively).

The net charge on NP (measured in the elementary charge units e) depends on its position z with respect to the grafting surface and can be expressed as

$$Q(z) = \sum_{i+} N_{i+}\alpha_{i+}(z) - \sum_{i-} N_{i-}\alpha_{i-}(z) \tag{19}$$

while the NP charge in the buffer is given by

$$Q_b = Q(z = \infty) = \sum_{i+} N_{i+}\alpha_{bi+} - \sum_{i-} N_{i-}\alpha_{bi-} \tag{20}$$

The isoelectric point, pH_{IEP}, corresponds to pH_b at which the NP charge in the buffer vanishes, $Q_b = 0$.

We focus primarily on the case of $pH_b \geq pH_{IEP}$, that is, when the NP in the bulk of the solution is charged negatively,

https://doi.org/10.1021/acs.biomac.2c01153
Biomacromolecules XXXX, XXX, XXX−XXX

$Q_b \leq 0$, i.e., similarly to the brush. Because the electrostatic potential $\psi(z)$ created by the brush is a monotonically increasing function of z (i.e., monotonically increasing in absolute value upon approaching the grafting surface), the net charge of the NP $Q(z)$ monotonically increases upon approaching the grafting surface and, depending on the sets of parameters $\{N_{i\pm}, K_{i\pm}\}$, $\{c_s, \mathrm{pH}_b\}$, $\{\alpha, \mathcal{N}, \sigma\}$, may remain negative or invert its sign to positive at some particular distance z^* from the grafting surface, so that

$$Q(z = z^*) = 0$$

Remarkably, z^* may correspond to the NP position either inside, or outside the brush (close to its edge). The position z^* can be found from the equation

$$\psi(z^*) = -\Delta\mathrm{pH}_b/\log_{10} e \approx -2.3\Delta\mathrm{pH}_b \quad (21)$$

with

$$\Delta\mathrm{pH}_b = \mathrm{pH}_b - \mathrm{pH}_{\mathrm{IEP}}$$

which implies (with the account of eq 18) that local $\mathrm{pH}(z = z^*)$ at $z = z^*$ coincides with $\mathrm{pH}_{\mathrm{IEP}}$ for NP in solution. Using eqs 13 and 19, one can demonstrate that

$$\left(\frac{\partial \Delta F_{\mathrm{ion}}(z)}{\partial z}\right)_{z^*} = 0 \quad (22)$$

that is, the ionization free energy passes through a maximum at $z = z^*$, i.e., in the point of the charge inversion. Indeed,

$$\frac{\partial \Delta F_{\mathrm{ion}}(z)}{\partial z} = \frac{\partial \Delta F_{\mathrm{ion}}}{\partial \lambda}\cdot\frac{\partial \lambda(z)}{\partial z}$$

where $\lambda(z) \equiv \exp(\psi(z))$. By taking the derivative of the r.h.s. of eq 13 with respect to $\lambda(z)$ (with the account of eqs 14 and 15), one arrives at

$$\frac{\partial \Delta F_{\mathrm{ion}}(z)}{\partial z} = \frac{1}{\lambda}\frac{\partial \lambda(z)}{\partial z}\cdot Q(z) = \frac{\partial \psi(z)}{\partial z}\cdot Q(z) \quad (23)$$

where the position-dependent charge $Q(z)$ of NP is given by eq 19. As soon as $\lambda(z)$ is a positive, monotonously increasing function of z in the whole range of $z \in [0, \infty)$, eq 23 indicates that $\Delta F_{\mathrm{ion}}(z)$ exhibits a maximum in the NP charge inversion point, $z = z^*$.

When $\Delta F_{\mathrm{ion}}(z = 0) \leq 0$ and $z^* \geq 0$, absorption of NP by the brush is thermodynamically favorable, and the minimum in $\Delta F_{\mathrm{ion}}(z)$ (reached at the grafting surface, $z = 0$) is separated from the exterior solution by the potential barrier with the height $\Delta F_{\mathrm{ion}}(z^*)$ located at $z = z^*$. As we demonstrate below, the charge inversion may occur at $z = z^* \geq 0$ even when $\Delta F_{\mathrm{ion}}(z = 0) \geq 0$. In this case, the localization of positively charged NP inside polyanionic brush corresponds to a metastable state. Finally, when z^* decreases down to zero, the charge inversion inside the brush does not take place and the insertion free energy $\Delta F_{\mathrm{ion}}(z)$ becomes a monotonically decreasing function of z. As a result, the Coulomb force pushes NP out of the brush and no absorption of NPs by PE brush occurs spontaneously.

Obviously, if NP is charged positively in the solution, $Q_b \geq 0$, then $\Delta F_{\mathrm{ion}}(z) \leq 0$ at $\forall z \in [0,\infty)$ and is a monotonically increasing function, $\partial \Delta F_{\mathrm{ion}}(z)/\partial z \geq 0\ \forall\ z \in [0, \infty)$.

3.2. Osmotic Contribution to the Free Energy. The second term in eq 4 accounts for the work against excess osmotic pressure of mobile ions inside the brush and in the double electrical layer outside. If the concentrations of mobile monovalent ions of low molecular weight salt in the buffer (at $z = \infty$) are $c_{b+} = c_{b-} = c_s$, then their concentrations at arbitrary distance z from the grafting surface are given by the Boltzmann law,

$$c_{\pm}(z) = c_s\ \exp(\mp\psi(z)) \quad (24)$$

and the excess osmotic pressure is

$$\Pi(z)/k_BT = c_+(z) + c_-(z) - 2c_s = \quad (25)$$

$$c_s(\exp(\psi(z)/2) - \exp(-\psi(z)/2))^2 = 4c_s\ \sinh^2(\psi(z)/2) \quad (26)$$

Hence, the osmotic contribution to the insertion free energy,

$$\Delta F_{\mathrm{vol}}(z)/k_BT = 4Vc_s\ \sinh^2(\psi(z)/2) \quad (27)$$

is proportional to NP volume V and monotonically decreases with z. Hence, the derivative of this second term in the free energy in eq 4 always provides a thermodynamic force expelling the NP from the brush.

We remark that in sufficiently dense or/and weakly charged brushes the nonelectrostatic (excluded volume) interactions provide the dominant contribution to the osmotic pressure.[37−39] However, in the present work we focus at sufficiently strongly charged brushes in which the electrostatic interactions dominate over the short-range repulsions between monomer units.

3.3. NP with Two Types of Ionizable Sites. Below we focus on a particular case when the NP comprises one type of cationic groups with ionization constant K_+ and one type of anionic groups with the ionization constant K_-. This simplification allows us to analyze the main trends in NP interaction with PE brush at variable environmental conditions (pH_b and c_s) and NP volume V.

The fraction of positively charged ionizable monomer units is defined as

$$f_+ = \frac{N_+}{N_- + N_+} \equiv \frac{N_+}{N_\Sigma} \quad (28)$$

where $N_+ + N_- = N_\Sigma$ is the total number of ionizable (basic and acidic) groups, and the ionic contribution ΔF_{ion} in eq 13 with $i_+ = i_- = 1$ reduces to

$$\Delta F_{\mathrm{ion}}(z)/k_BT = N_\Sigma\left[f_+\ \ln\left(\frac{1-\alpha_+(z)}{1-\alpha_{b+}}\right) + (1-f_+)\ln\left(\frac{1-\alpha_-(z)}{1-\alpha_{b-}}\right)\right] \quad (29)$$

In section 3.3.1, we start with the analysis of $\Delta F_{\mathrm{ion}}(z)$, which is the dominant contribution to the overall free energy, $\Delta F(z) \approx \Delta F_{\mathrm{ion}}(z)$, in the case of small NPs. In the following section 3.3.2 we consider the interplay between $\Delta F_{\mathrm{ion}}(z)$ and $\Delta F_{\mathrm{vol}}(z)$ which becomes essential for increasingly bulky charged species and may prevent NP absorption by PE brush even if the reionization free energy, ΔF_{ion}, provides a driving force for it.

3.3.1. Reionization Free Energy for NP Interacting with Polyelectrolyte Brush. Below we present typical ionization free energy profiles $\Delta F_{\mathrm{ion}}(z)$ normalized by the total number of ionizable sites N_Σ calculated for the NP with $f_+ = 0.5$ at varied pH_b, reduced salt concentration $C_s = c_s a^3$ and grafting density $\sigma = a^2/s$. We use model equal values of ionization constants $\mathrm{p}K_- = \mathrm{p}K_+ = 5$ that assures maximal impact of the reionization

https://doi.org/10.1021/acs.biomac.2c01153
Biomacromolecules XXXX, XXX, XXX−XXX

free energy to the overall insertion free energy balance and corresponds at $f_+ = 0.5$ to the IEP $pH_{IEP} = 5$. In real experiment chosen parameters are sufficiently close to the pK_- value for carboxylic groups and not far from pK_+ value for, e.g., $N(CH_3)_2$ groups.

The degree of polymerization of the brush-forming chains $\mathcal{N} = 300$. Notably, C_s and σ affect the magnitude of the excess electrostatic potential created by the brush, whereas pH_b controls degrees of ionization of the cationic and anionic residues and the net charge of the globule Q_b in the buffer.

In Figure 2a,b, the position-dependent free energy $\Delta F_{ion}(z)$ and charge $Q(z)$ are plotted as a function of distance z from the grafting surface for a series of pH_b values at constant salt concentration $C_s = 10^{-3}$.

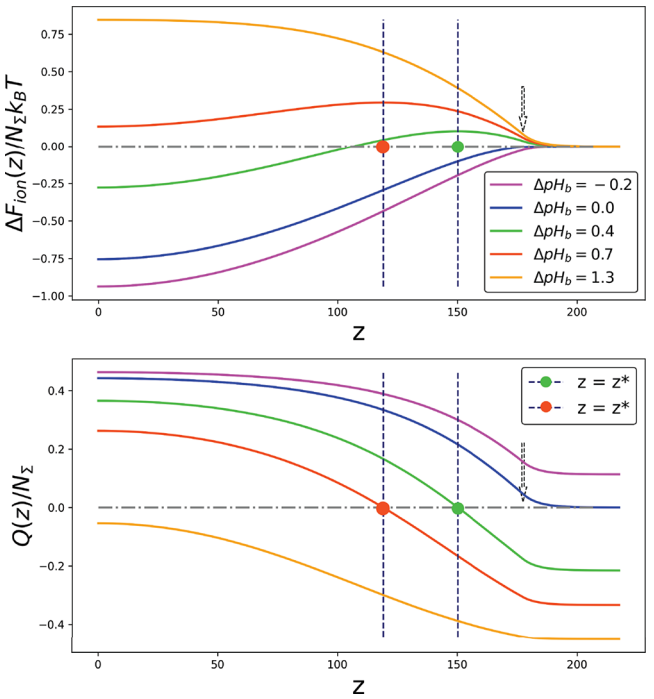

Figure 2. Position-dependent insertion free energy $\Delta F_{ion}(z)$ (a) and the NP charge $Q(z)$ (b) both normalized by N_Σ, as a function of the distance z from the grafting surface for a series of pH_b values around the IEP at fixed salt concentration $C_s = 10^{-3}$. Arrows indicate the upper boundary of the brush. Dashed vertical lines indicate the charge inversion point, $z = z^*$. Dashdot horizontal lines indicate $\Delta F_{ion}(z) = 0$ and $Q(z) = 0$. Colored circles in panels (a) and (b) correspond to the charge inversion points $z = z^*$.

In Figure 3a,b, we show cross sections of 2D profiles of the insertion free energy $\Delta F_{ion}(z, \Delta pH_b)$, and net charge $Q(z, \Delta pH_b)$ of the NP plotted at three selected values of salt concentration C_s

As one can see from Figures 2b and 3b and follows from eq 19, because of reionization of cationic and anionic sites in the electrostatic potential of the polyanionic brush, net charge $Q(z)$ of the NP is always a decreasing function of z.

Sufficiently far above the IEP (e.g., at $\Delta pH_b = 1.3$ in Figure 2a,b), the NP is negatively charged in the buffer and remains negatively charged, $Q(z) \leq 0\ \forall z \in [0,\infty)$, though $|Q(z)|$ decreases in the absolute value upon insertion of the NP into the brush. The insertion free energy in this case is positive, $\Delta F_{ion}(z) > 0\ \forall z \in [0,\infty)$, and monotonously decreasing

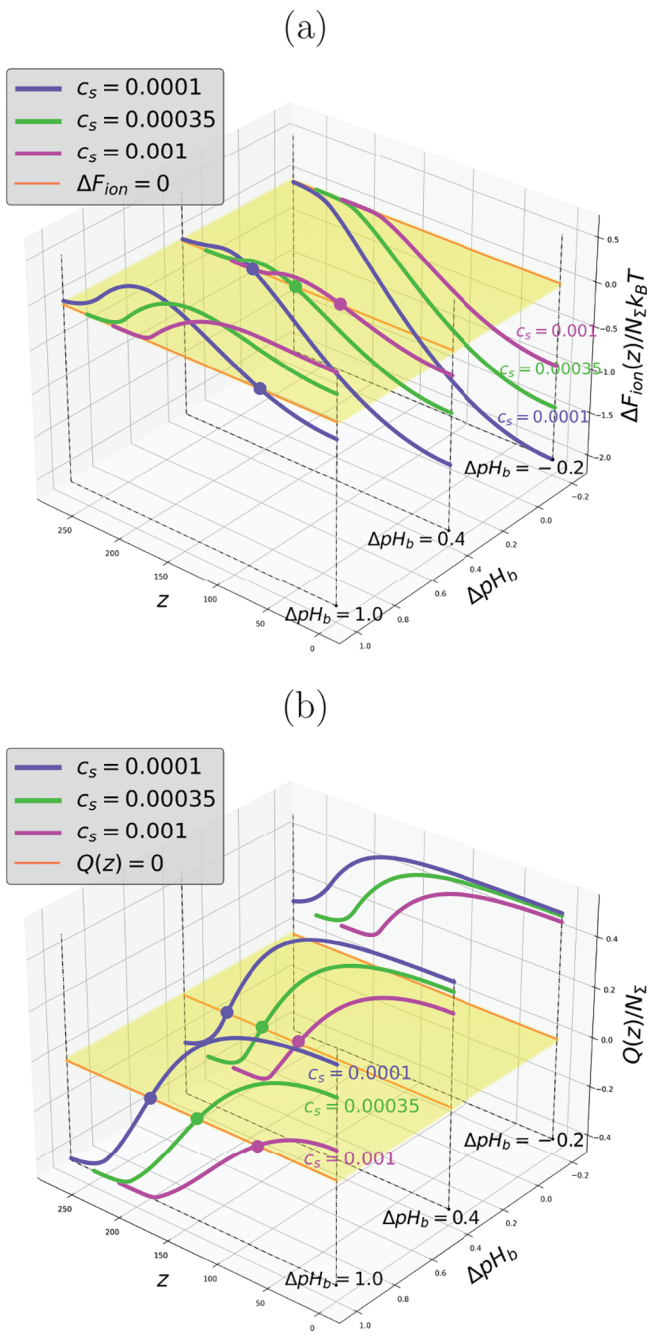

Figure 3. Cross sections of the 2D profiles of the insertion free energy $\Delta F_{ion}(z, \Delta pH_b)$ (a) and NP charge $Q(z, \Delta pH_b)$ (b), both normalized by N_Σ, for a set of values of salt concentration (with the corresponding color code, as indicated at the curves). Colored circles in panel (a) indicate points of vanishing free energy, $\Delta F_{ion}(z, \Delta pH_b) = 0$; colored circles in panel (b) correspond to the charge inversion points $z = z^*$.

function of z, $\partial \Delta F_{ion}(z)/\partial z \leq 0$, that is, the NP is expelled from the brush.

On the contrary, below the IEP, at $\Delta pH_b < 0$, the charge of the NP is positive, $Q(z) > 0\ \forall z \in [0,\infty)$ (Figures 2b and 3b). The free energy $\Delta F_{ion}(z) < 0\ \forall z \in [0, \infty)$ is negative and monotonously decreases upon approaching the grafting surface (Figures 2a and 3a). In this case, the NP and the brush are oppositely charged, and the NP is driven into the brush by the attractive Coulomb force. The depth of the free energy edge minimum at the grafting surface, $\Delta F_{ion}(z = 0)$, grows upon a

https://doi.org/10.1021/acs.biomac.2c01153
Biomacromolecules XXXX, XXX, XXX−XXX

decrease in ΔpH_b, or upon an increase in the magnitude of the negative electrostatic potential at the surface which can be induced either by a decrease in salt concentration C_s (Figure S2a) or by an increase in grafting density σ (Figure S2b). The same applies also at the IEP, pH = pH_{IEP}, when the NP charge is vanishing far away from the brush, but becomes positive and monotonously increases when NP approaches and enters the brush.

The most peculiar patterns in $\Delta F_{ion}(z)$ and $Q(z)$ are observed at $\Delta pH_b \geq 0$, i.e., slightly above the IEP, as illustrated by Figure 2a,b and the cross-section of the $\Delta F_{ion}(z, \Delta pH_b)$ surface at $\Delta pH_b = 0.4$ in Figure 3a,b. In this case NP is charged negatively in the buffer, $Q_b < 0$, but inverts the sign of its charge upon embedding into the brush at $z = z^*$. That is, the NP charge $Q(z \geq z^*) \leq 0$ and $Q(z \leq z^*) \geq 0$. As demonstrated above, the free energy $\Delta F_{ion}(z)$ passes through a maximum in the charge inversion point $z = z^*$, i.e., $\Delta F_{ion}(z)$ is an increasing function of z at $z \in [0, z^*)$ and a decreasing function of z at $z \in [z^*, \infty)$. Obviously, $z^* \to \infty$ at $pH_b \to pH_{IEP}$.

In Figure 4 we present a typical zoomed profile of the free energy $\Delta F_{ion}(z)$ with maximum, corresponding to the $Q(z)$

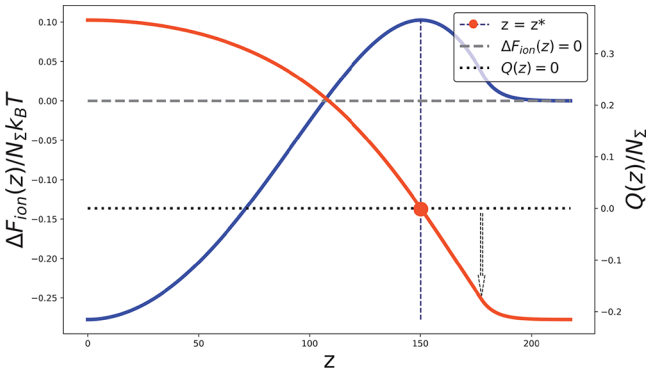

Figure 4. Characteristic dependence of the $\Delta F_{ion}(z)$ with a maximum at $z = z^*$ and corresponding dependence $Q(z)$ with charge inversion at $z = z^*$ plotted for $\Delta pH_b = 0.4$ both normalized by N_Σ. Salt concentration is $C_s = 10^{-3}$, grafting area per chain is $s/a^2 = 100$. Arrow indicate the upper boundary of the brush ($z = H$), and the charge inversion point $z = z^*$ is indicated by vertical dashed line and a red circle.

sign inversion point, and $\Delta F_{ion}(z = 0) < 0$. This free energy profile indicates the presence of electrostatic driving force for NP absorption by PE brush.

Remarkably, similar patterns in the position-dependent net charge were observed in Molecular Dynamic simulations[27] of ampholytic oligopeptide interacting with strongly charged starlike polyelectrolyte: in the vicinity of the IEP the oligopeptide charge inversion was observed upon approaching the center of the star. However, quantitative comparison of our results to those presented in ref[27] is challenging because of essentially different spatial distribution of polymer density and electrostatic field in a planar PE brush and in a single PE star.

As seen in Figure 3a,b, an increase in salt concentration (at a given ΔpH_b) leads to the shift in the charge inversion point z^* toward the grafting surface, the decrease in $Q(z)$, and narrowing of the presurface potential well which simultaneously becomes more shallow.

Upon a moderate increase in pH_b above the IEP, i.e., upon a decrease in the NP charge $Q_b < 0$ in the buffer, the charge inversion point z^* is shifted toward the grafting surface, the magnitude of the maximum in $\Delta F_{ion}(z)|_{z=z^*}$ increases, and the depth of the presurface potential well, $|\Delta F_{ion}(z = 0)|$, decreases. In this regime, absorption of NPs by the brush remains thermodynamically favorable, but requires overcoming of the potential barrier with maximum at $z = z^*$. At sufficiently large number of ionizable groups on NP surface, $N_\Sigma \sim 10^2$, the barrier may increase up to $\sim 10 k_B T$ thus completely hindering NP absorption by PE brush kinetically.

When ΔpH_b exceeds the threshold value $\Delta pH_b^{(abs)} \geq 0$ (that is, pH_b exceeds $pH_b^{(abs)} > pH_{IEP}$), the free energy $\Delta F_{ion}(z)$ becomes positive at $\forall z \in [0, \infty)$. The free energy minimum at $z = 0$ remains separated from the bulk of the solution by the potential barrier located at $z = z^*$. Hence, the NP location inside the brush at $0 \leq z \leq z^*$ corresponds to a metastable state although the globule possesses positive net charge, $Q(z \leq z^*) \geq 0$ (see, e.g., the curves corresponding to $\Delta pH_b = 0.7$ in Figure 2a,b). Indeed, the local free energy minimum at $z = 0$ is separated from the global free energy minimum $\Delta F_{ion}(z = \infty) = 0$ by a potential barrier at $z = z^*$, which implies that, by definition,[40] the position of the NP in the brush corresponds not to an equilibrium, but to a metastable state.

Further increase in pH_b results in simultaneous increase in the magnitude of the potential barrier at $z = z^*$ and its displacement toward the grafting surface and concomitant decrease in the depth and width of the potential well. Eventually, $z^* \to 0$, and the free energy $\Delta F_{ion}(z)$ becomes a positive and monotonously decreasing function of z, so that the NP−PE brush interaction becomes purely repulsive.

Because the position-dependent net charge $Q(z)$ and the free energy $\Delta F_{ion}(z)$ depend on the brush local electrostatic potential $\psi(z)$, both properties are strongly affected by salt concentration in the buffer. The magnitude of $\psi(z)$ decreases, and its range shrinks as the salt concentration in the buffer increases (see Figure S2a in the Supporting Information). Therefore, the equilibrium absorption threshold can be crossed also by an increase in the salt concentration at constant pH_b, as demonstrated by series of the cross sections of the $\Delta F_{ion}(z, \Delta pH_b)$ surfaces corresponding to $\Delta pH_b = 1.0$ and different values of C_s in Figure 3a,b. For given set of parameters $\{f_+, K_+, K_-\}$ the defined above threshold $pH_b^{(abs)}$ depends on salt concentration C_s, as demonstrated in Figure 5.

In Figure 6a,b, we present $\Delta F_{ion}(z)$ and $Q(z)$ profiles for a number of selected salt concentrations C_s and constant $\Delta pH_b = 0.3$. In Figure 7a,b, we show cross sections of 2D profiles of the insertion free energy $\Delta F_{ion}(z, c_s)$, and net charge $Q(z, c_s)$ of the NP plotted at three selected values of ΔpH_b above the IEP. The values of pH_b are chosen sufficiently close to pH_{IEP} so that, at low salt concentration, $C_s = 10^{-3}$, the $\Delta F_{ion}(z)$ exhibits pronounced maxima at the charge inversion points and the edge minima at $z = 0$.

An increase in salt concentration leads to weakening of the electrical field created by PE brush, and the magnitude of the electrostatic potential $|\psi(z = 0)|$ decreases. Upon an increase in salt concentration, the charge inversion point $z = z^*$ is shifted to a smaller z, the free energy at the grafting surface, $\Delta F_{ion}(z = 0)$, increases, changes its sign from negative to positive, and $\Delta F_{ion}(z)$ acquires a monotonously decreasing shape corresponding to expulsion of NPs from PE brush. The larger the ΔpH_b, the smaller the salt concentration is needed to suppress charge inversion and eliminate the potential well at the grafting surface.

https://doi.org/10.1021/acs.biomac.2c01153
Biomacromolecules XXXX, XXX, XXX−XXX

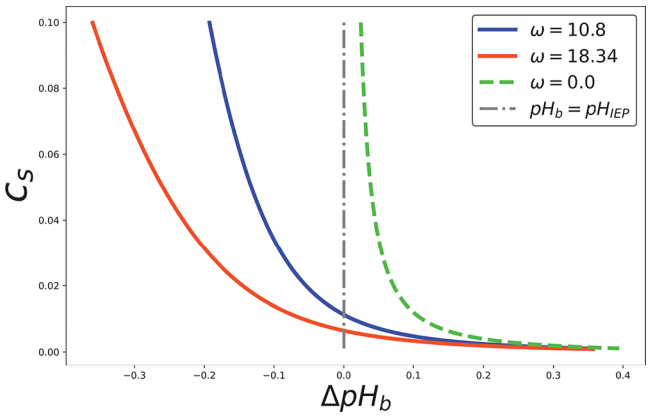

Figure 5. Dependences of salt concentration $C_s^{(max)}$ corresponding to inversion of sign of $\Delta F_{ion}(z = 0)$ (dashed line) and $C_s^{(max,\omega)}$ corresponding to inversion of sign of $\Delta F_{ion}(z = 0) + \Delta F_{vol}(z = 0)$ (solid lines) for selected values of ω (see color code in the figure) on deviation ΔpH_b from the IEP.

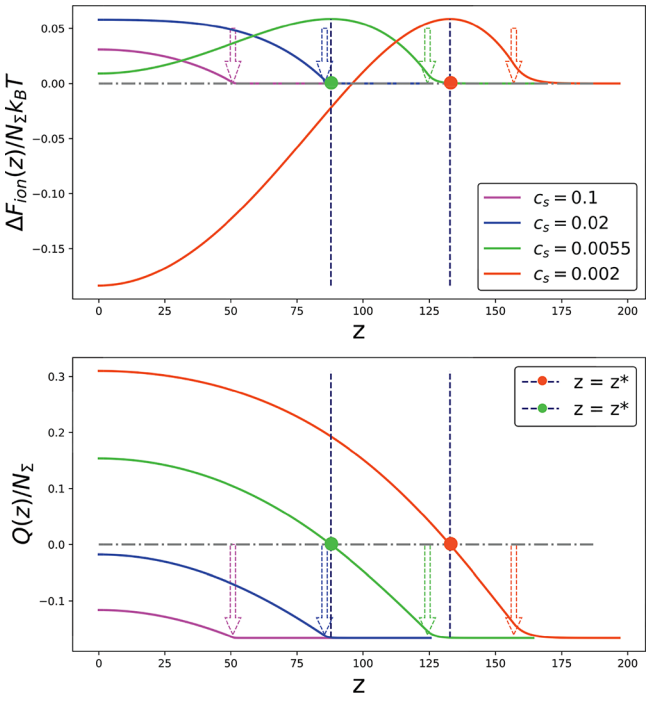

Figure 6. Position-dependent insertion free energy $\Delta F_{ion}(z)$ (a) and the NP charge $Q(z)$ (b), both normalized by N_Σ, as a function of the distance z from the grafting surface for a series of salt concentration C_s values at $\Delta pH_b = 0.3$. Arrows indicate the salt-dependent position of the upper boundary of the brush. Dashed vertical lines indicate the charge inversion points, $z = z^*$. Dashdot horizontal lines indicate $\Delta F_{ion}(z) = 0$ and $Q(z) = 0$. Colored circles in panels (a) and (b) correspond to the charge inversion points $z = z^*$.

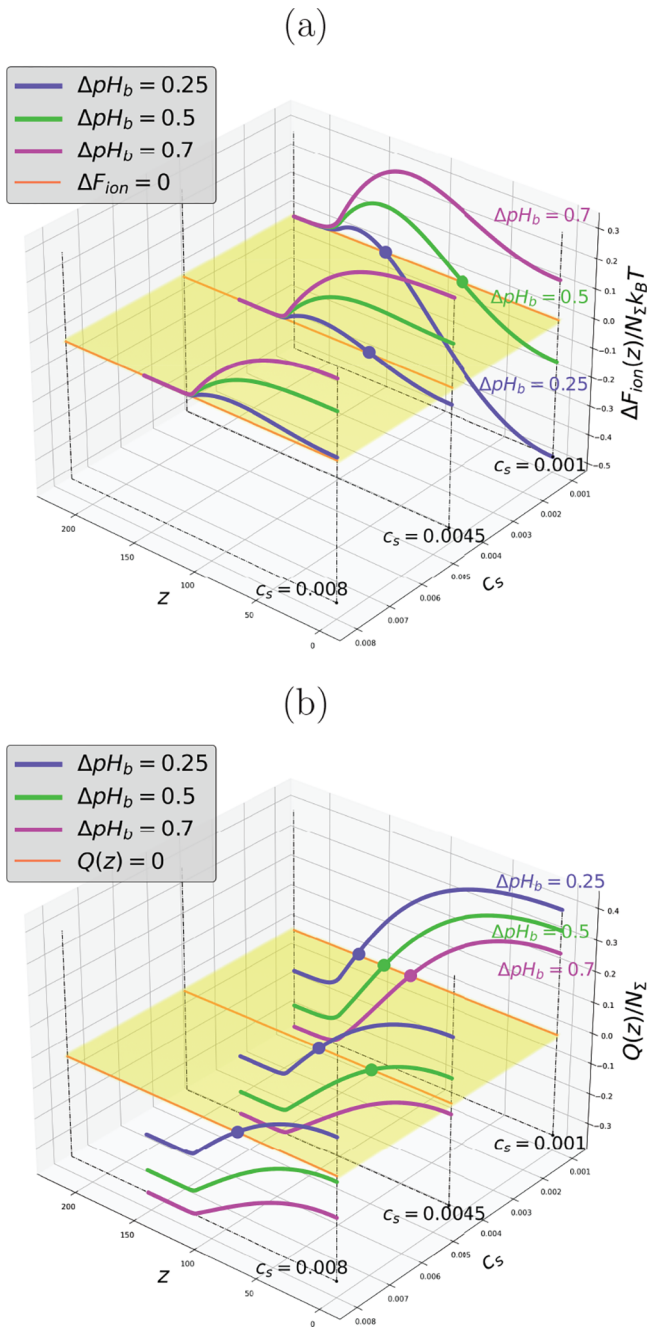

Figure 7. Cross sections of the 2D profiles of the insertion free energy $\Delta F_{ion}(z, c_s)$ (a) and NP charge $Q(z, c_s)$ (b), both normalized by N_Σ, for a set of values of pH_b (with the corresponding color code, as indicated at the curves). Colored circles in panel (a) indicate points of vanishing free energy, $\Delta F_{ion}(z, \Delta pH_b) = 0$; colored circles in panel (b) correspond to the charge inversion points $z = z^*$.

Remarkably, if $\Delta pH_b > 0$ and $Q|_{z=0} < 0$ or, on the contrary, $\Delta pH_b < 0$ and $Q|_{z=0} > 0$, the addition of salt does not lead to qualitative changes in the shape of the $\Delta F_{ion}(z)$ curves: They are monotonously decreasing or monotonically increasing in the former and in the latter case, respectively, but their magnitudes (the height of the potential barrier or the depth of the potential well) as well as the range of the potential (proportional to the brush thickness H) decrease.

The effect of the grafting density $\sigma = a^2/s$ on the $\Delta F_{ion}(z)$ curves is illustrated by Figure 8: An increase in the grafting density enhances electrostatic potential, causes additional stretching of the brush-forming PE chains (an increase in the brush thickness H) and might drive NP absorption into sufficiently dense PE brush.

3.3.2. Interplay between NP Charge and Volume. For an ampholytic NP (protein globule) the ionic contribution to the insertion free energy $\Delta F_{ion}(z)$ is complemented by the osmotic term $\Delta F_{vol}(z)$. In this subsection we unravel the competitive effects of the electrostatic (attractive) and osmotic (repulsive) forces on NP absorption by PE brush.

https://doi.org/10.1021/acs.biomac.2c01153
Biomacromolecules XXXX, XXX, XXX−XXX

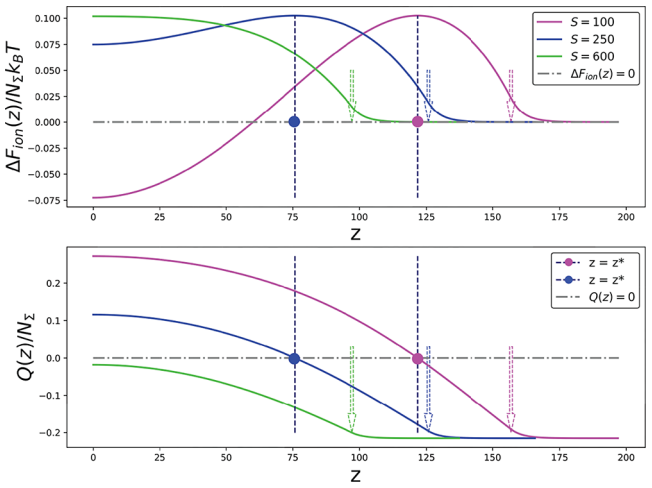

Figure 8. Position-dependent insertion free energy $\Delta F_{ion}(z)$ (a) and the NP charge $Q(z)$ (b) both normalized by N_Σ, as a function of the distance z from the grafting surface for a series of $s = a^2/\sigma$ values at $C_s = 10^{-3}$, $\Delta pH_b = 0.4$ (with the corresponding color code, as indicated at the curves). Arrows indicate the upper boundary of the brush. Dashed vertical lines indicate the charge inversion point, $z = z^*$. Dashdot horizontal lines indicate $\Delta F_{ion}(z) = 0$ and $Q(z) = 0$. Colored circles in panels (a) and (b) correspond to the charge inversion points $z = z^*$.

While the ionic part of the insertion free energy, $\Delta F_{ion}(z)$, may exhibit different patterns as a function of z, the osmotic contribution $\Delta F_{vol}(z)$ given by eq 27 is always a positive and monotonously decreasing function of z. As a result, at $\Delta pH_b > 0$ and $\Delta F_{ion}(z) > 0$ at any $z \geq 0$, the net free energy is positive, $\Delta F(z) = \Delta F_{ion}(z) + \Delta F_{vol}(z) > 0$ as well, and NP absorption by PE brush is unfavorable. Even when the ionic interactions provide a driving force for globule absorption, (i.e., $\Delta F_{ion}(z = 0) < 0$), the net insertion free energy $\Delta F(z = 0)$ may be still positive due to the osmotic term, $\Delta F_{vol}(z = 0)$, overcompensating the attractive ionic contribution.

Using eqs 4, 27, and 29, the NP insertion free energy can be presented as

$$\Delta F(z) = N_\Sigma \left(\left[f_+ \ln\left(\frac{1-\alpha_+(z)}{1-\alpha_{b+}}\right) + (1-f_+)\ln\left(\frac{1-\alpha_-(z)}{1-\alpha_{b-}}\right)\right] + 4\omega C_s \sinh^2(\psi(z)/2)\right) \quad (30)$$

where we have introduced the following parameter

$$\omega = V/a^3 N_\Sigma \quad (31)$$

which is equal to the average globule volume per ionizable group. Because $\Delta F_{ion}(z) \sim N_\Sigma$ (eq 29) and $\Delta F_{vol}(z) \sim V$ (eq 27), the relative strength of the osmotic and ionic contributions, $\Delta F_{vol}/\Delta F_{ion}$, depends on the parameter ω. Remarkably, ω is an increasing function of the globule dimensions (since N_Σ does not grow faster than the globule surface area Σ).

In Table 1 we list approximate estimates of the parameter ω for a number of globular proteins, using values of V and N_Σ from the literature.[41] Notably, the values of ω in Table 1 constitute lower boundaries, since all the ionizable residues (not necessarily located at the globule surface) have been accounted for in the corresponding protein.

Table 1. Proteins Corresponding to the ω Coefficient

ω	name of the protein
2.0	human serum albumin
3.2	Des-Phe B1 bovine insulin
3.5	phospholipase A2 (PLA2) from Naja naja venom
3.7	α-lactalbumin
4.9	human interleukin-6
5.3	human hemoglobin A2
6.1	human sex hormone-binding globulin
7.5	interleukin-37
8.6	bovine β-lactoglobulin
10.3	bromoperoxidase A1
15.7	human interleukin-17A
29.2	pumpkin seed globulin

For given globule volume V, $\Delta F_{vol}(z)$ in eq 27 (as well as $|\psi(z)|$ in eqs 5 and 9) is a decreasing function of salt concentration c_s in the buffer, and an increasing function of the brush grafting density $\sigma = a^2/s$.

Consider first the scenario when $\Delta pH_b \geq 0$, and the $\Delta F_{ion}(z)$ curve exhibits a characteristic pattern with the maximum at $z = z^*$ and the minimum at the grafting surface, $\Delta F_{ion}(z = 0) \leq 0$. In this case, the ionic interactions provide a driving force for the globule absorption above IEP, accompanied by the NP charge reversal. In Figure 9a we illustrate the evolution of the insertion free energy profile, $\Delta F(z) = \Delta F_{ion}(z) + \Delta F_{vol}(z)$, upon an increase in the parameter ω. As one can see in Figure 9a, at small values of ω (NPs with relatively small volume V and large number N_Σ of ionizable groups) the $\Delta F(z)$ curve has the same shape as $\Delta F_{ion}(z)$. That is, exhibits a maximum close to the edge of the

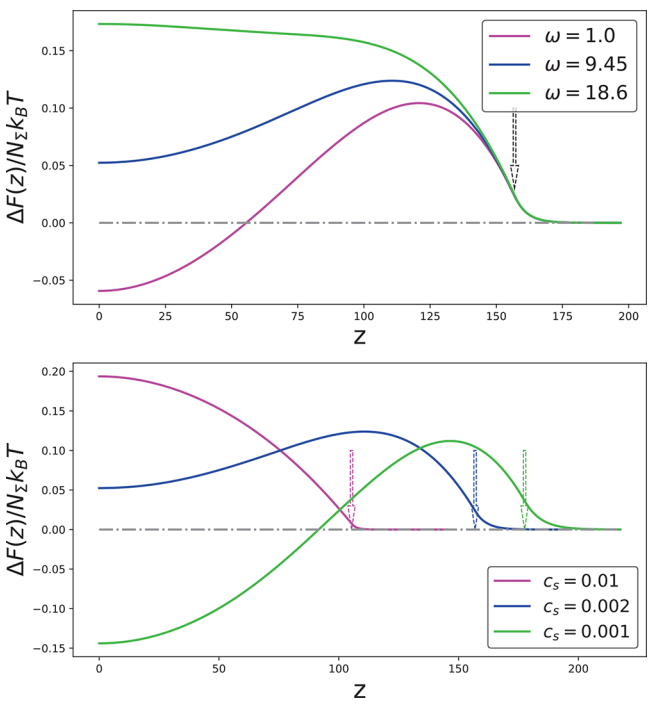

Figure 9. Total free energy curves $\Delta F(z) = \Delta F_{ion}(z) + \Delta F_{vol}(z)$ normalized by N_Σ corresponding to different globule volume to the number of charge ratio ω at $C_s = 0.002$ (a) and at fixed $\omega = 9.45$ and varied salt concentration C_s (b). Other parameters are $s/a^2 = 100$. The brush boundary, $z = H$, is indicated by the arrows. Dashdot horizontal lines indicate $\Delta F(z) = 0$.

https://doi.org/10.1021/acs.biomac.2c01153
Biomacromolecules XXXX, XXX, XXX−XXX

brush and reaches a negative value at the grafting surface, but with the curve as a whole moving upward. Importantly, position of the maximum, $z = z_{max}$, is shifted toward the grafting surface with respect to z^* ($z_{max} \leq z^*$), and does not correspond anymore to the globule charge inversion threshold (i.e., $Q(z = z_{max}) > 0$). Further increase in the globule volume V (i.e., an increase in ω) results in further shift of the maximum toward the grafting surface, and the increase in both, $\Delta F(z_{max})$ and $\Delta F(z = 0)$. The latter becomes eventually positive indicating that the osmotic repulsion overcompensates the electrostatic attraction making globule absorption thermodynamically unfavorable. At large ω, $\Delta F(z)$ become a monotonously decreasing function of z with $\Delta F(z) > 0$ at any $z \geq 0$.

An increase in salt concentration leads to the simultaneous decrease in both, the electrostatic driving force for NP absorption and the osmotic repulsion, and eventually suppresses the globule absorption by PE brush (as seen in Figure 9b). The combined effects of the NP volume-to-charge ratio ω and salt concentration c_s are illustrated also by cross sections of the 2D profiles of the insertion free energy curves, f10 $\Delta F(z, c_s)$ and $\Delta F(z, \omega)$, presented in Figure 10a and b, respectively. Remarkably, an increase in ω or/and in salt concentration c_s leads to the decrease in depth of the minimum in $\Delta F(z)$ (and, eventually, its disappearance), but does not affect its position at $z = 0$.

As it follows from our analysis, only small protein globules with large number of ionizable groups are efficiently absorbed by PE brushes at $\Delta pH_b \geq 0$, while bigger ones are not (unless other driving forces are involved).

We now examine the interplay between forces of electrostatic attraction and osmotic repulsion in the case $\Delta pH_b \leq 0$, i.e., when $Q(z) \geq 0$ at any $z \geq 0$. The free energy profiles $\Delta F(z)$ corresponding to progressively increasing values of ω f11f12 are presented in Figure 11a and Figure 12a. They demonstrate qualitatively new trends compared to the case $\Delta pH_b \geq 0$. For example, at $\omega = 15$ the ionic contribution to the free energy dominates, $\Delta F(z) \leq 0$ at any z, and thermodynamically most favorable position of the globule is close to the grafting surface. An increase in ω leads to the shift of the whole $\Delta F(z)$ curve upward and change in its shape: The repulsive osmotic contribution becomes dominant close to the grafting surface, so that $\Delta F(z = 0)$ becomes positive, and a potential well develops at the periphery of the brush where the negative ionic contribution $\Delta F_{ion}(z) < 0$ dominates over the osmotic repulsion. The width and the depth of the potential well decrease upon an increase in ω, and its position is shifted to the edge of the brush. Eventually, at large ω the peripheral potential well disappears, and $\Delta F(z)$ becomes a monotonously decreasing function of z, indicating expulsion of globules from PE brush.

Another trend is observed at $\Delta pH_b \leq 0$ if ω is small and kept constant, but the salt concentration increases, Figures 11b and 12b: Notably the magnitudes of both electrostatic (negative) and osmotic (positive) contributions to the free energy diminish upon an increase in salt concentration C_s. At very low salt concentration the electrostatic attraction dominates over osmotic repulsion at any distance from the surface and $\Delta F(z)$ is a monotonously increasing function of z. At higher salt concentrations, the osmotic (repulsive) part of the free energy starts to dominate in the proximal to the grafting surface region, while in the distal region ($z \approx H$) the electrostatic attraction, $\Delta F_{ion}(z)$, provides the dominant

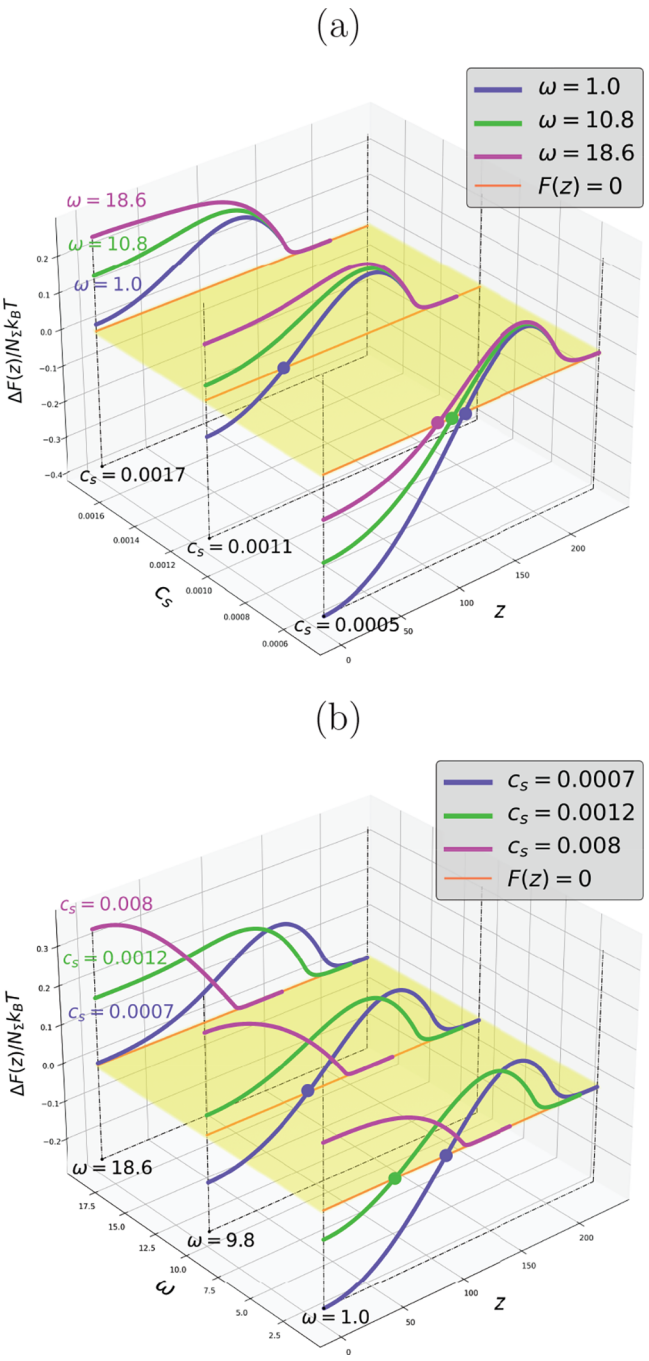

Figure 10. Cross sections of the 2D profiles of the total free energy curves $\Delta F(z, c_s) = \Delta F_{ion}(z, c_s) + \Delta F_{vol}(z, c_s)$ (a) and $\Delta F(z, \omega) = \Delta F_{ion}(z, \omega) + \Delta F_{vol}(z, \omega)$ (b), both normalized by N_Σ, for a set values of ω corresponding to different globule volume to the number of charges ratio (a) and different salt concentrations (b) (with the corresponding color code, as indicated at the curves). $s/a^2 = 100$. Colored circles in panels indicate points of vanishing free energy, $\Delta F(z, c_s) = 0$ and $\Delta F(z, \omega) = 0$.

contribution to $\Delta F(z)$. As a result, a minimum in $\Delta F(z)$ develops in the distal region. The depth of this minimum decreases and its position z_{min} is shifted toward the grafting surface upon an increase in salt concentration and a concomitant decrease in the brush thickness H. Hence, when the osmotic contribution to the free energy becomes comparable to the ionic one due to sufficiently large globule volume or high salt concentration, the insertion free energy

https://doi.org/10.1021/acs.biomac.2c01153
Biomacromolecules XXXX, XXX, XXX−XXX

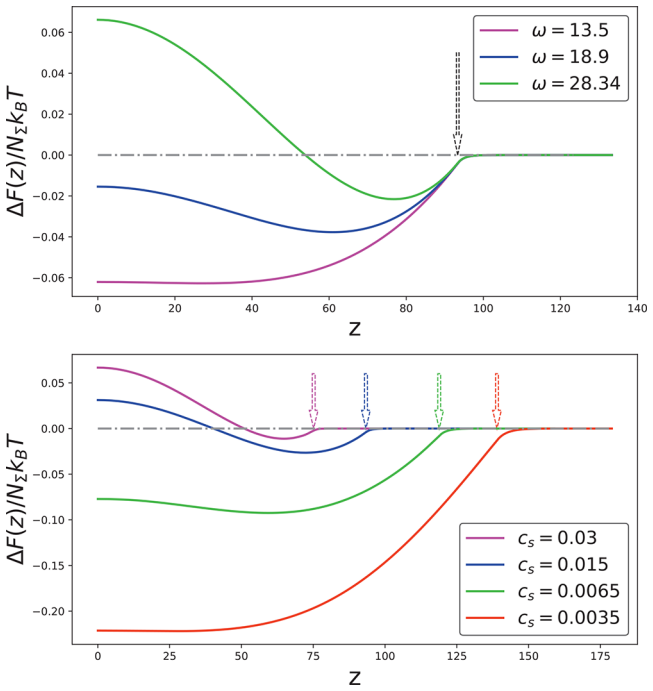

Figure 11. Total free energy curves $\Delta F(z) = \Delta F_{ion}(z) + \Delta F_{vol}(z)$ normalized by N_Σ, at different globule volume to the number of charges raio ω. C_s = 0.015 (a) and at ω = 24.3 and varied salt concentration (b). The brush boundary, $z = H$, is indicated by the arrows. Dashdot horizontal lines indicate $\Delta F(z) = 0$.

curves decrease from $\Delta F(z = 0) \geq 0$ in the proximal to the grafting surface region and pass through a minimum (with $\Delta F(z = z_{min}) \leq 0$) localized in the distal region of the brush.

Solid lines in the diagram in Figure 5 correspond to the salt concentration $C_s^{(max,\omega)}$ separating regimes $\Delta F(0) \leq 0$ (absorption) and $\Delta F(0) > 0$ (repulsion). As follows from Figure 5, this boundary is systematically displaced toward lower salt concentration when ω (the globule bulkiness) increases.

4. CONCLUSIONS

In this paper we have applied the analytical self-consistent field Poisson−Boltzmann approach to study thermodynamics of interactions between planar PE brushes and globular proteins, modeled as nanoparticles (NPs) comprising weak cationic and anionic groups on their surfaces. The position-dependent insertion free energy $\Delta F(z)$ and the net charge $Q(z)$ of the NP were calculated as a function of environmental conditions (pH and salt concentration c_s in the buffer), numbers of cationic and anionic ionizable groups on the NP surface, the NP volume V, and grafting density σ of the brush-forming polyelectrolyte chains.

The insertion free energy $\Delta F(z) = \Delta F_{ion}(z) + \Delta F_{vol}(z)$ accounts for the position-dependent ionization contribution $\Delta F_{ion}(z)$ of NP in the electrostatic field induced by a planar PE brush, and for the work $\Delta F_{vol}(z)$ performed against excess osmotic pressure of mobile ions. As long as the electrostatic potential $\psi(z)$ induced by permanently charged ("quenched") PE brush can be tuned by changing the ionic strength in the solution, $\Delta F_{vol}(z)$ is controlled solely by the globule volume V and the salt concentration c_s in the buffer. On the contrary, $\Delta F_{ion}(z)$ can be expressed as a function of ionization degrees of cationic, $\alpha_+(z)$ and anionic, $\alpha_-(z)$ groups that depend on both,

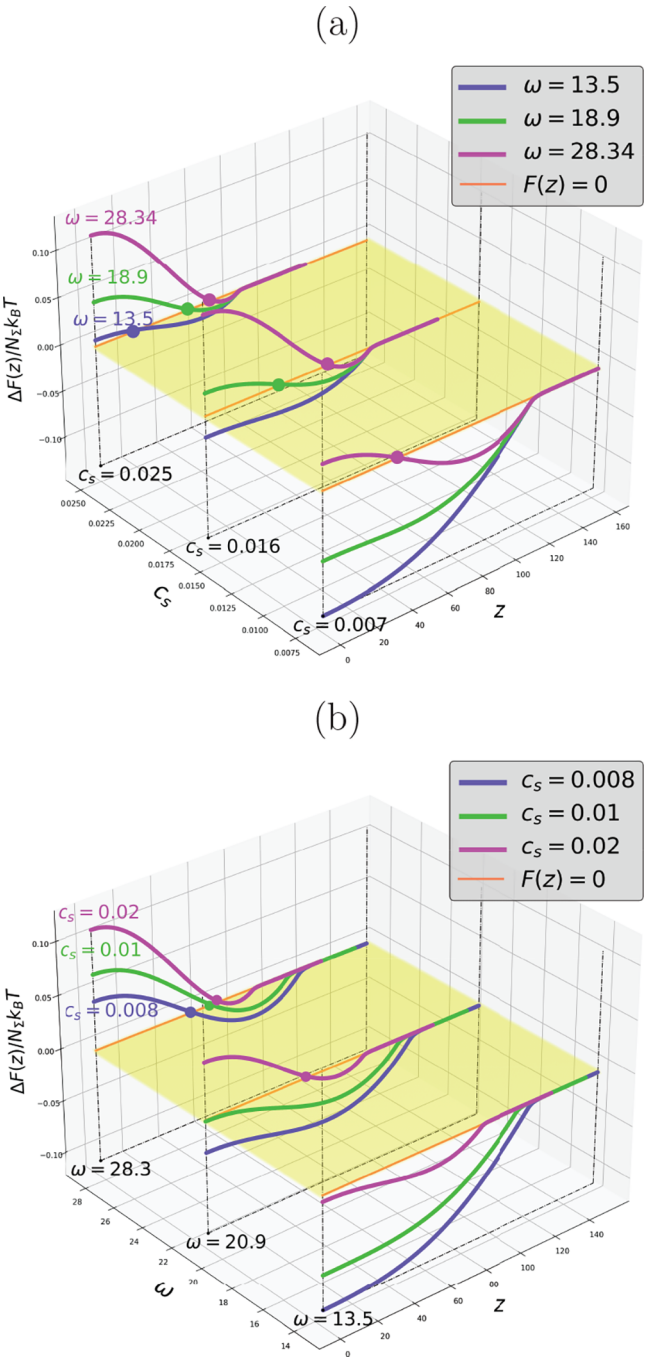

Figure 12. Cross sections of the 2D profiles of the total free energy curves $\Delta F(z, c_s) = \Delta F_{ion}(z, c_s) + \Delta F_{vol}(z, c_s)$ (a) and $\Delta F(z)(z, \omega) = \Delta F_{ion}(z, \omega) + \Delta F_{vol}(z, \omega)$ (b), both normalized by N_Σ for a set values of ω corresponding to different globule volume to the number of charges ratio (a) and different salt concentrations (b), respectively (with the corresponding color code, as indicated at the curves). s/a^2 = 100. Colored circles in panels indicate points of vanishing free energy, $\Delta F(z, c_s) = 0$ and $\Delta F(z, \omega) = 0$.

the buffer pH_b, and the ionic strength (via $\psi(z)$). Importantly, $\alpha_-(z)$ decreases providing positive contribution to $\Delta F_{ion}(z)$, whereas $\alpha_+(z)$ increases providing negative contribution to $\Delta F_{ion}(z)$ upon insertion of NP in polyanionic brush (with the electrostatic potential $\psi(z) \leq 0$ monotonously increasing as a function of z). Generalization to the case of polycationic PE brush is straightforward by changing sign of $\psi(z)$ from negative to positive.

https://doi.org/10.1021/acs.biomac.2c01153
Biomacromolecules XXXX, XXX, XXX−XXX

In calculating the insertion free energy $\Delta F(z)$ we implemented a number of approximations:

(i) An uptake of NPs (protein globules) from buffer solution by PE brush is presumed to occur without changing the conformational state of the globule and spatial distribution of electrostatic potential $\psi(z)$ induced by the brush. That is, NPs are considered as probes. This approximation is valid at small protein concentrations $c_b^{(\text{globules})}$ in buffer solution, and at no strong binding of NPs to the brush-forming PE chains.

(ii) Small values of $c_b^{(\text{globules})} \ll 1$ allow us to specify the density profiles $c^{(\text{globules})}(z)$ of absorbed in the brush globules as

$$c^{(\text{globules})}(z) = c_b^{(\text{globules})} \exp[-\Delta F(z)] \tag{32}$$

and the related partition coefficient,

$$\frac{\langle c^{(\text{globules})} \rangle}{c_b^{(\text{globules})}} = \frac{1}{H}\int_0^H \exp[-\Delta F(z)]\mathrm{d}z \tag{33}$$

The latter specifies the ratio of average concentration $\langle c^{(\text{globules})} \rangle$ of globules inside the brush, and concentration $c_b^{(\text{globules})}$ in the buffer solution. The limitation $c_b^{(\text{globules})} \ll 1$ is most important at $\text{pH}_b \leq \text{pH}_{\text{IEP}}$ when absorption of large amounts of NPs by colloidal polyelectrolyte brushes unavoidably leads to collapse of the brush and loss of colloid stability. This restriction is less important if PE chains are grafted to planar substrates, although perturbation of the PE brush structure upon absorption of large amounts of NPs also brings the theory to the limit of its validity.

(iii) Reionization upon insertion is assumed to occur for all N_Σ ionizable groups on NP. However, for globular proteins with compact ternary structure, only amino acid residues localized at the globule-water interlace are involved in (re)ionization process, leading therefore to concomitant renormalization of N_Σ.

(iv) Our approach does not account for additional attraction between NP and PE brush due to charge−charge correlations that provide negative contribution to the insertion free energy $\Delta F(z)$. The charge−charge correlations are most important for protein globules with pronounced nonuniform ("patchy") distribution of cationic and anionic groups on the globule surface. In the latter case, the brush-forming PE chains may adsorb on the oppositely charged patches of charge, but be depleted from similarly charged patches.[24]

(v) Our model neglects also the short-range nonelectrostatic interactions between the brush-forming PE chains and the surface of NPs that could be mediated by the solvent quality or temperature. In spite of the anticipated dominant role of electrostatic forces, such interactions should be necessarily taken into account for full quantitative prediction of absorption threshold and diffusion rates for specific proteins.

By implementing the above approximations, and using the self-consistent Poisson−Boltzmann approach, we have demonstrated that the insertion free energy profiles $\Delta F(z)$ exhibit complex patterns as a function of z depending on the environmental conditions (pH_b, c_s) and the globule volume V normalized by the number of ionizable groups N_Σ. The depth of the minima and the height of the maxima in $\Delta F(z)$ profiles are mediated by the number N_Σ of ionizable groups, and the globule volume V. Notably, the implemented approach allows us to specify the lower pH_b boundary for uptake of NPs by PE brush.

The analysis of our results indicates that one can distinguish three characteristic ranges of pH_b with respect to the NP isoelectric point, pH_{IEP}, in the buffer:

$\text{pH}_b > \text{pH}_{\text{IEP}}$. The NP is strongly negatively charged in the buffer, $Q_b < 0$. The NP charge Q remains negative upon insertion in polyanionic brush, but decreases in magnitude upon approach to the grafting surface, where the electrostatic potential of PE brush is the strongest. The $\Delta F_{\text{ion}}(z)$ and $\Delta F(z)$ are monotonously decreasing functions of z indicating expulsion of NPs from the brush. The magnitude of the repulsive free energy grows as a function of pH_b (due to the increase in $|Q_b|$), but decreases upon an increase in the ionic strength in the buffer solution.

$\text{pH}_b \geq \text{pH}_{\text{IEP}}$. The NP is charged negatively in the buffer, $Q_b \leq 0$, but acquires positive net charge upon insertion (or approach to PE brush). The charge inversion, $Q(z) = 0$, occurs at $z = z^*$ at which $\Delta F_{\text{ion}}(z)$ passes through a maximum. At $z \leq z^*$ the globule charge becomes positive and keeps increasing whereas the ionic part of the free energy, $\Delta F_{\text{ion}}(z)$, decreases reaching either positive or negative value at the grafting surface, $z = 0$. For small globules, $\Delta F(0) < 0$ indicates their accumulation in the brush. At $\Delta F(0) > 0$, the local minimum in $\Delta F_{\text{ion}}(z)$ at the grafting surface, $z = 0$, corresponds to a metastable state separated by the potential barrier from the bulk of the solution. Hence, even when the NP net charge changes its sign from negative to positive, absorption of NPs by PE brush is not necessarily thermodynamically favorable though NPs may be kinetically trapped there.

An increase in the ionic strength of the solution weakens the electrostatic potential $\psi(z)$ and hinders reionization of anionic and cationic groups of the inserted in the brush NP. As a result, the charge inversion point, z^*, and the corresponding maximum in $F_{\text{ion}}(z)$ are displaced toward the grafting surface (where the magnitude of $\psi(z)$ is larger), the free energy $\Delta F_{\text{ion}}(z = 0)$ grows and turns from negative to positive indicating passing the absorption threshold. Eventually, at high salt concentrations the potential $\psi(z)$ becomes too weak to induce reionization of the NP inside the brush, and the NPs are repelled by the brush.

A progressive increase in the NP volume V (an increase in ω) at constant ionic strength leads to the growth of repulsive osmotic contribution $\Delta F_{\text{vol}}(z)$ at constant $\Delta F_{\text{ion}}(z)$. As a result, the $\Delta F(z)$ curves are shifted upward while the position of maximum, z_{max}, is displaced toward the grafting surface. Importantly, now the position of maximum, z_{max}, does not coincide with the charge inversion point, z^*, and $Q(z = z_{\text{max}}) \geq 0$. Further increase in the NP volume V leads to $\Delta F(z = 0) \geq 0$ and eventual transformation of $\Delta F(z)$ into monotonously decreasing curve. That is, expulsion of the bulky globule from the brush in spite of the charge inversion (which can be traced in the $\Delta F_{\text{ion}}(z)$ and $Q(z)$ curves).

$\text{pH}_b \leq \text{pH}_{\text{IEP}}$. The NP is positively charged in the buffer and, therefore, attracted to the PE brush by the Coulomb force. The $\Delta F_{\text{ion}}(z) \leq 0$ at all z, and the NP positive charge grows upon insertion into the brush and approach to the grafting surface. However, absorption of a bulky globule can be hindered and even fully suppressed due to osmotic (repulsive) term, $\Delta F_{\text{vol}}(z)$. An increase in the globule volume (and in

https://doi.org/10.1021/acs.biomac.2c01153
Biomacromolecules XXXX, XXX, XXX−XXX

$\Delta F_{vol}(z)$) at constant salt concentration c_s leads to the increase in $\Delta F(z)$ primarily in the proximal to the grafting surface region, flattening of the presurface potential well, and eventually leading to the appearance of the presurface maximum with $\Delta F(z = 0) \geq 0$. The maximum is separated from the bulk of the solution by the minimum which progressively gets more shallow and narrow, and is displaced to the external boundary of PE brush. A similar evolution of $\Delta F(z)$ curve is observed for globules with fixed V and N_Σ upon variations in the salt concentration. The minimum in $\Delta F(z)$ is shifted toward the periphery of the brush (and progressively disappears) upon an increase in c_s. The theory thereby predicts that below IEP the interplay between ionic attraction and osmotic repulsion may result in preferential accumulation of the absorbed protein globules in the central or even peripheral regions of the brush, whereas the proximal to the grafting surface region is depleted from globules. This feature is most attractive in design of bionanoreactors in which accumulation of the proteins (enzymes) in the brush is required, but their direct contacts with underlying substrate (that could lead to nonspecific adsorption, denaturation, and loss of enzymatic activity) should be avoided.

We remark that amplitudes of the minima and maxima in $\Delta F(z)$ curves that determine the thermodynamic stability of the protein absorbed state or the probability of overcoming the potential barrier separating the absorbed state from the bulk of the solution or from the grafting surface depend on the number of charged groups and volume of the globule. With typical values of $N_\Sigma \sim 10^2$, the potential well easily reaches the depth of a few k_BT under experimentally relevant conditions. Furthermore, reionization and the NP absorption on the "wrong side" of the IEP is suppressed by increasing salt concentration (in full agreement with the experimental data[20]), but might be operational for sufficiently densely grafted PE brushes that induce strong local electrostatic field.

To summarize, our theory predicts how the electrostatic and osmotic parts of the insertion free energy change upon insertion of ampholytic NP containing pH-sensitive acidic and basic groups in a planar PE brush from the solution in a wide range of the buffer pH_b. On the "wrong side" of the isoelectric point, the negative balance in the free energy may be assured by overcompensation of the free energy losses due to suppression of ionization of similarly (with respect to the brush) charged monomeric groups by gains due to enhanced ionization of the oppositely charged ones, and be accompanied by the change in the sign of the net charge of NP inside the brush. However, the local minimum in the NP free energy inside the brush may correspond to a metastable state even if it is accompanied by the net charge reversal. Importantly, knowledge of the insertion free energy profile $\Delta F(z)$ allows also for the calculation and control of the diffusion rates of NPs through the brush to be considered in our forthcoming publication.

■ ASSOCIATED CONTENT

Supporting Information

The Supporting Information is available free of charge at https://pubs.acs.org/doi/10.1021/acs.biomac.2c01153.

Detailed derivation of the electrostatic potential distribution in the planar PE brush (PDF)

■ AUTHOR INFORMATION

Corresponding Author

Oleg V. Borisov − *CNRS, Université de Pau et des Pays de l'Adour UMR 5254, Institut des Sciences Analytiques et de Physico-Chimie pour l'Environnement et les Matériaux, 64053 Pau, France; St. Petersburg National Research University of Information Technologies, Mechanics and Optics, 197101 St. Petersburg, Russia; Institute of Macromolecular Compounds of the Russian Academy of Sciences, 199004 St. Petersburg, Russia;* orcid.org/0000-0002-9281-9093; Email: oleg.borisov@univ-pau.fr

Authors

Tatiana O. Salamatova − *St. Petersburg National Research University of Information Technologies, Mechanics and Optics, 197101 St. Petersburg, Russia;* orcid.org/0000-0002-7559-1824

Mikhail Y. Laktionov − *St. Petersburg National Research University of Information Technologies, Mechanics and Optics, 197101 St. Petersburg, Russia*

Ekaterina B. Zhulina − *Institute of Macromolecular Compounds of the Russian Academy of Sciences, 199004 St. Petersburg, Russia;* orcid.org/0000-0001-9139-3484

Complete contact information is available at: https://pubs.acs.org/10.1021/acs.biomac.2c01153

Notes

The authors declare no competing financial interest.

■ ACKNOWLEDGMENTS

This work was financially supported by Russian Foundation for Basic Research, Grant 21-53-10005.

■ REFERENCES

(1) Achazi, K.; Haag, R.; Ballauff, M.; Dernedde, J.; Kizhakkedathu, J. N.; Maysinger, D.; Multhaup, G. Understanding the Interaction of Polyelectrolyte Architectures with Proteins and Biosystems. *Angew. Chem., Int. Ed.* **2021**, *60* (8), 3882−3904.

(2) Nie, C. A. X.; Pouyan, P.; Lauster, D.; Trimpert, J.; Kerkhoff, Y.; Szekeres, G. P.; Wallert, M.; Block, S.; Sahoo, A. K.; Dernedde, J.; Pagel, K.; Kaufer, B. B.; Netz, R. R.; Ballauff, M.; Haag, R. Polysulfates Block SARS-CoV-2 Uptake through Electrostatic Interactions. *Angew. Chem., Int. Ed.* **2021**, *60* (29), 15870−15878.

(3) Kapelner, R. A.; Yeong, V.; Obermeyer, A. C. Molecular determinants of protein-based coacervates. *Curr. Opin. Colloid Interface Sci.* **2021**, *52*, 101407.

(4) Yeong, V.; Werth, E. G.; Brown, L. M.; Obermeyer, A. C. Formation of biomolecular condensates in bacteria by tuning protein electrostatics. *ACS Cent. Sci.* **2020**, *6*, 2301−2310.

(5) Kabanov, A. V.; Kabanov, V. A. Interpolyelectrolyte and block ionomer complexes for gene delivery: physico-chemical aspects. *Adv. Drug Delivery Rev.* **1998**, *30* (1−3), 49−60.

(6) Schallon, A.; Synatschke, C. V.; Jerome, V.; Müller, A. H. E.; Freitag, R. Nonpartiulate Nonviral Agent for the Effective Delivery of pDNA and si RNA to Differentiated Cells and Primary Human T Lymphocytes. *Biomacromolecules* **2012**, *13*, 3463−3474.

(7) Miyata, K.; Nishiyama, N.; Kataoka, K. Rational design of smart supramolecular assemblies for gene delivery: chemical challenges in the creation of artificial viruses. *Chem.Soc. Rev.* **2012**, *41*, 2562−2574.

(8) Yu, T.; Liu, X.; Bolcato-Bellemin, A.-L.; Wang, Y.; Liu, C.; Erbacher, P.; Qu, F.; Rocchi, P.; Behr, J.-P.; Peng, L. An amphiphilic dendrimer for effective delivery of small interfering RNA and gene silencing in vitro and in vivo. *Angew. Chem., Int. Ed.* **2012**, *124*, 8606−8612.

(9) Liu, X.; Zhou, J.; Yu, T.; Chen, C.; Cheng, Q.; Sengupta, K.; Huang, Y.; Li, H.; Liu, C.; Wang, Y.; Posocco, P.; Wang, M.; Cui, Q.; Giorgio, S.; Fermeglia, M.; Qu, F.; Pricl, S.; Shi, Y.; Liang, Z.; Rocchi, P.; Rossi, J. J.; Peng, L. Adaptive Amphiphilic Dendrimer-Based Nanoassemblies as Robust and Versatile siRNA Delivery Systems. *Angew. Chem., Int. Ed.* **2014**, *126*, 12016−12021.
(10) Fan, X.; Zhao, Y.; Xu, W.; Li, L. Linear-Dendritic Block Copolymer for Drug and Gene Delivery. *Mater. Sci. Eng., C* **2016**, *62*, 943−959.
(11) Malmsten, M.; Bysell, H.; Hansson, P. Biomacromolecules in Microgels - Opportunities and Challenges for Drug Delivery. *Curr. Opin. Colloid Interface Sci.* **2010**, *15*, 435−444.
(12) Bysell, H.; Mansson, R.; Hansson, P.; Malmsten, M. Microgels and Microcapsules in Peptide and Protein Drug Delivery. *Adv. Drug Delivery Rev.* **2011**, *63*, 1172−1185.
(13) Hachim, D.; Whittaker, T. E.; Kim, H.; Stevens, M. M. Glycosaminoglycan-based biomaterials for growth factor and cytokine delivery: Making the right choices. *J. Controlled Release* **2019**, *313*, 131−147.
(14) Braatz, D.; Dimde, M.; Ma, G.; Zhong, Y.; Tully, M.; Grotzinger, C.; Zhang, Y.; Mavroskoufis, A.; Schirner, M.; Zhong, Z.; Ballauff, M.; Haag, R. Toolbox of Biodegradable Dendritic (Poly glycerol sulfate)-SS-poly(ester) Micelles for Cancer Treatment: Stability, Drug Release, and Tumor Targeting. *Biomacromolecules* **2021**, *22* (6), 2625−2640.
(15) Kiani, C.; Chen, L.; Wu, Y. J.; Yee, A. J.; Yang, B. B. Structure and functions of aggrecan. *Cell Res.* **2002**, *12*, 19−32.
(16) Cagno, V.; Tseligka, E. D.; Jones, S. T.; Tapparel, C. Heparan sulfate proteoglycans and viral attachment: True receptors or adaptation bias? *Viruses* **2019**, *11* (7), 596.
(17) Wittemann, A.; Haupt, B.; Ballauff, M. Adsorption of proteins on spherical polyelectrolyte brushes in aqueous solution. *Phys. Chem. Chem. Phys.* **2003**, *5*, 1671−1677.
(18) Wittemann, A.; Ballauff, M. Interaction of proteins with linear polyelectrolytes and spherical polyelectrolyte brushes in aqueous solution. *Phys. Chem. Chem. Phys.* **2006**, *8*, 5269−5275.
(19) Becker, A. L.; Henzler, K.; Welsch, N.; Ballauff, M.; Borisov, O. V. Proteins and polyelectrolytes: A charge relationship. *Curr. Opin. Colloid Interface Sci.* **2012**, *17*, 90−96.
(20) Walkowiak, J.; Gradzielski, M.; Zauscher, S.; Ballauff, M. Interaction of Proteins with a Planar Poly(acrylic acid) Brush: Analysis by Quartz Crystal Microbalance with Dissipation Monitoring (QCM-D). *Polymers* **2021**, *13*, 122.
(21) Yigit, C.; Welsch, N.; Ballauff, M.; Dzubiella, J. Protein Sorption to Charged Microgels: Characterizing Binding Isotherms and Driving Forces. *Langmuir* **2012**, *28*, 14373−14385.
(22) Biesheuvel, P. M.; Wittemann, A. A modified box model including charged polyelectrolyte brush: self-consistent field theory. *J.Phys.Chem. B* **2005**, *109*, 4209−4214.
(23) de Vos, W. M.; Leermakers, F. A. M.; de Keizer, A.; Cohen Stuart, M. A.; Kleijn, J. M. Field theoretical analysis of driving forces for the uptake of proteins by like-charge polyelectrolyte brushes: effects of charge regulation and patchiness. *Langmuir* **2010**, *26*, 249−259.
(24) Leermakers, F. A. M.; Ballauff, M.; Borisov, O. V. On the mechanisms of interaction of globular proteins with polyelectrolyte brushes. *Langmuir* **2007**, *23*, 237−247.
(25) Xu, X.; Angioletti-Uberti, S.; Lu, Y.; Dzubiella, J.; Ballauff, M. Interaction of Proteins with Polyelectrolytes: Comparison of Theory to Experiment. *Langmuir* **2019**, *35*, 5373−5391.
(26) Kim, S.; Sureka, H. V.; Kayitmazer, A. B.; Wang, G.; Swan, J. W.; Olsen, B. D. Effect of protein surface charge distribution on protein-polyelectrolyte complexation. *Biomacromolecules* **2020**, *21*, 3026−3037.
(27) Lunkad, R.; Barroso da Silva, F. L.; Kosovan, P. Both Charge-Regulation and Charge-Patch Distribution Can Adsorption on the Wrong Side of the Isoelectric Point. *J. Am. Chem. Soc.* **2022**, *144*, 1813−1825.
(28) Laktionov, M. Y.; Zhulina, E. B.; Borisov, O. V. Proteins and polyampholytes interacting with polyelectrolyte brushes and microgels: the charge reversal concept revised. *Langmuir* **2021**, *37*, 2865−2873.
(29) Zhulina, E. B.; Borisov, O. V. Structure and Interactions of Weakly Charged Polyelectrolyte Brushes: Self-Consistent Field Theory. *textit J. Chem. Phys.* **1997**, *107*, 5952−5967.
(30) Zhulina, E. B.; Klein Wolterink, J.; Borisov, O. V. Screening Effects in Polyelectrolyte Brush: Self-Consistent Field Theory. *Macromolecules* **2000**, *33*, 4945−4953.
(31) Lebedeva, I. O.; Zhulina, E. B.; Borisov, O. V. Self-consistent Field Theory of Polyelectrolyte Brushes with Finite Chain Extensibility. *J. Chem. Phys.* **2017**, *146*, 214901−6.
(32) Zhulina, E. B.; Borisov, O. V. Poisson-Boltzmann Theory of pH-Sensitive (Annealing) Polyelectrolyte Brush. *Langmuir* **2011**, *27*, 10615−10633.
(33) Zhulina, E. B.; Borisov, O. V. Brushes of Dendritically Branched Polyelectrolytes. *Macromolecules* **2015**, *48* (19), 1499−1508.
(34) Zhulina, E. B.; Boulakh, A. B.; Borisov, O. V. Repulsive Forces between Spherical Polyelectrolyte Brushes in Salt-Free Solution. *Z. Phys. Chem. (Berlin, Ger.)* **2012**, *226*, 625−643.
(35) Lunkad, R.; Murmiliuk, A.; Tosner, Z.; Stepanek, M.; Kosovan, P. Role of pKA in Charge Regulation and Conformation of Various Peptide Sequences. *Polymers* **2021**, *13*, 214.
(36) Lunkad, R.; Biehl, P.; Murmiliuk, A.; Blanco, P. M.; Mons, P.; Stepanek, M.; Schacher, F. H.; Kosovan, P. Simulations and Potentiometric Titrations Enable Reliable Determination of Effective pK_a Values of Various Polyzwitterions. *Macromolecules* **2022**, *55*, 7775−7784.
(37) Halperin, A.; Kröger, M.; Zhulina, E. B. Colloid-brush interactions: The effect of solvent quality. *Macromolecules* **2011**, *44*, 3622−3638.
(38) Merlitz, H.; Wu, C.-X.; Sommer, J.-U. Inclusion Free Energy of Nanoparticles in Polymer Brushes. *Macromolecules* **2012**, *45*, 8494−8501.
(39) Laktionov, M. Y.; Shavykin, O. V.; Leermakers, F. A. M.; Zhulina, E. B.; Borisov, O. V. Colloidal particles interacting with a polymer brush: a self-consistent field theory. *Phys. Chem. Chem. Phys.* **2022**, *24*, 8463−8476.
(40) Landau, L. D.; Lifshitz, E. M. *Statistical Physics*; Pergamon Press: Oxford, 1986.
(41) RCSB PDB: Homepage. https://www.rcsb.org (accessed 2022−08−21).

https://doi.org/10.1021/acs.biomac.2c01153
Biomacromolecules XXXX, XXX, XXX−XXX